Cluster reveals the magnetospheric cusps

1: Artist's impression of the four Cluster spacecraft. (J Huart/ESA)

Benoit Lavraud and Peter J Cargill explain the structure of the magnetospheric cusps and their relationship with the solar wind, as revealed by Cluster data.

ABSTRACT

We report on the structure of the high-altitude cusp regions of the terrestrial magnetosphere, which has been the topic of numerous studies using the multispacecraft data from the ESA's Cluster mission. This summary of the 8 October 2004 RAS meeting focuses on the characteristics of the large-scale structure of these regions. We explore the role played by the cusps for solar wind plasma penetration and transport into the magnetosphere by examining the effects of the orientation of the interplanetary magnetic field (IMF) and of the occurrence of the magnetic reconnection process. We additionally emphasize, through the description of two selected techniques, the ability of the Cluster four-spacecraft measurements to resolve boundary dynamics and wave characteristics in an unprecedented fashion.

The overall nature of the interaction of the supersonic solar wind with the Earth's magnetic field is now quite familiar. The terrestrial magnetic field is an obstacle to the solar wind, which is decelerated and diverted at a bow shock located roughly 15 Earth radii (R_E) sunward, where $1\,R_E = 6370$ km. The shock gives rise to a hot plasma region, the magnetosheath, which has an interface with the Earth's magnetic field at the magnetopause (figures 2a, b). The magnetosphere is the cavity inside the magnetopause and arises due to the confinement of Earth's magnetic field by the solar wind. Because the magnetospheric field is dipolar, it possesses two singularities, corresponding to the northern and southern poles, where the topology of the magnetic field is not well defined. These are the magnetospheric cusps (figure 2).

The magnetic topology of the cusps makes them a prime site for solar wind plasma to enter the magnetosphere (see Heikkila and Winningham 1971 and Frank 1971 for early results). At low and middle altitudes (below $5\,R_E$), the cusps are well explored, extend between 1 and 2° in latitude and 1–2 hours in local time, and typically include low-energy solar-wind ions and electrons (Newell and Meng 1988). The cusps at high altitude near the magnetopause, especially their dependence on the interplanetary magnetic field (IMF), are only now being investigated fully using results from Cluster.

The European Space Agency Cluster mission was launched in the summer of 2000, and is unique. It comprises four identical satellites, each with 11 instruments that study plasmas and electromagnetic fields. It has a polar orbit (perigee of $4\,R_E$ and apogee of $19.6\,R_E$), and its line of apside is along the Sun–Earth direction. The spacecraft thus sample the high-altitude cusp and solar wind during spring and the mid-altitude cusp in summer and autumn (figs 2a and 2b). The average separation between the spacecraft varies from ~100 km to ~$1\,R_E$. They can form a tetrahedron configuration that is optimized in the high-altitude cusps.

After four years of Cluster operations, exploration of the high-altitude cusps has reached a mature level. To take stock of developments, a discussion meeting was organized under the auspices of the RAS on 8 October 2004, and was attended by many scientists from the UK and overseas. The following discussion presents an overview of the subject at this time rather than summaries of the talks. It focuses on the large-scale structure of the high-altitude cusp.

The role of magnetic reconnection

Prior to Cluster there was uncertainty as to what determined the overall cusp structure. Some workers proposed an "inward sag" or indentation of the magnetopause at the cusp, leading to a range of complex flows and shock waves (e.g. Paschmann *et al.* 1976, Haerendel *et al.* 1978, Cargill 1999). In contrast, Cluster results have established convincingly that many properties of the high-altitude cusp can be attributed to

magnetic reconnection processes at the magnetopause. The way that reconnection influences the cusp depends on the orientation of the IMF, as shown qualitatively in figures 3a and 3b.

For southward IMF, magnetic reconnection occurs at the subsolar magnetopause (labelled "X-line" on figure 3a). This leads to a large-scale convection electric field in the cusp region resulting in a "velocity filter" effect on the entering plasma (e.g. Lockwood and Smith 1992). The plasma mantle, at the poleward edge of the cusp, is formed by the tail of the dispersed cusp plasma and so contains mainly tailward and upflowing plasma. For northward IMF, sunward convection is present in the cusp, probably due to magnetic reconnection at the high-latitude magnetopause, tailward of the cusp. Under such conditions, the magnetosheath and magnetospheric fields are anti-parallel in the lobe region (labelled "X-line" in figure 3b). This northward IMF scenario should lead to the absence of a plasma mantle and a different large-scale plasma flow behaviour in the whole region.

Structure of plasma flow: statistical

The difference between these two scenarios can be seen through studies of individual cusp crossings and statistical surveys. A survey of three years of Cluster data in the high-altitude cusp has been undertaken using magnetic field and ion plasma data from the FluxGate Magnetometer (FGM) (Balogh *et al.* 2001) and Cluster Ion Spectrometer (CIS) (Rème *et al.* 2001) respectively. The aim was to establish global magnetic field and plasma properties of the high-altitude cusp and the nature of the boundaries with the surrounding regions as a function of IMF orientation (Lavraud *et al.* 2004a, b). Because the cusps respond readily to solar wind conditions, the technique accounts for cusp displacement and radial magnetopause motion.

Figure 4 shows the spatial distribution of the ratio of the measured magnetic pressure ($B^2/2\mu_0$) to that estimated from the Tsyganenko (1996: T96) semi-empirical vacuum magnetic field model. The distribution shows a transition region between the magnetosheath and magnetosphere that is referred to as the "exterior cusp". It is characterized by the presence of cold and dense plasma of solar wind origin (Lavraud *et al.* 2004a) resulting in a diamagnetic effect, leading to a region of depressed magnetic pressure when compared to the T96 model.

Using a combination of the magnetic field and plasma distributions, Cluster has shown, unambiguously, three distinct boundaries surrounding the exterior cusp (Lavraud *et al.* 2004a). Guidelines for their positions are shown by the red lines in figure 4 and they separate the exterior cusp from (a) the lobe at the poleward edge, (b) the dayside magnetosphere at the equatorward edge, and (c) the magnetosheath outward.

Figures 3c and d show the distributions of the

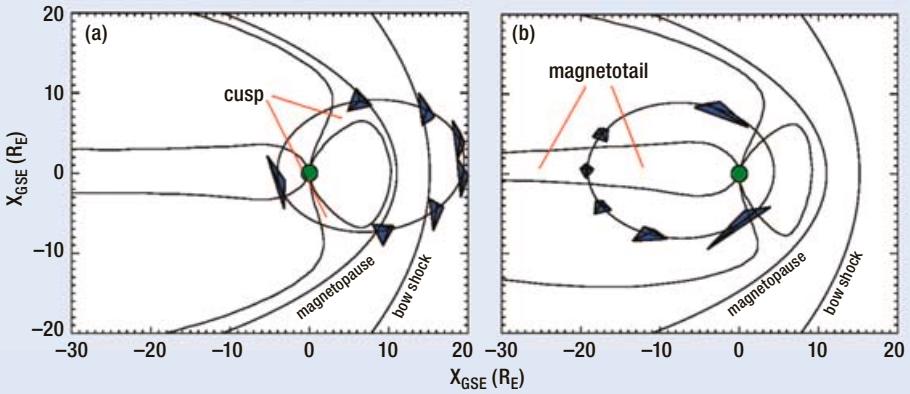

2: The Cluster orbit showing its passage through the different regions of the magnetosphere during the spring (a: left) and autumn (b: right) seasons. The Sun is located to the right of each panel and in this representation Cluster moves clockwise (counterclockwise) in spring (autumn). The topology of the tetrahedral spacecraft configuration is shown at a number of times. The high-altitude cusp is only sampled during spring (see text for further description).

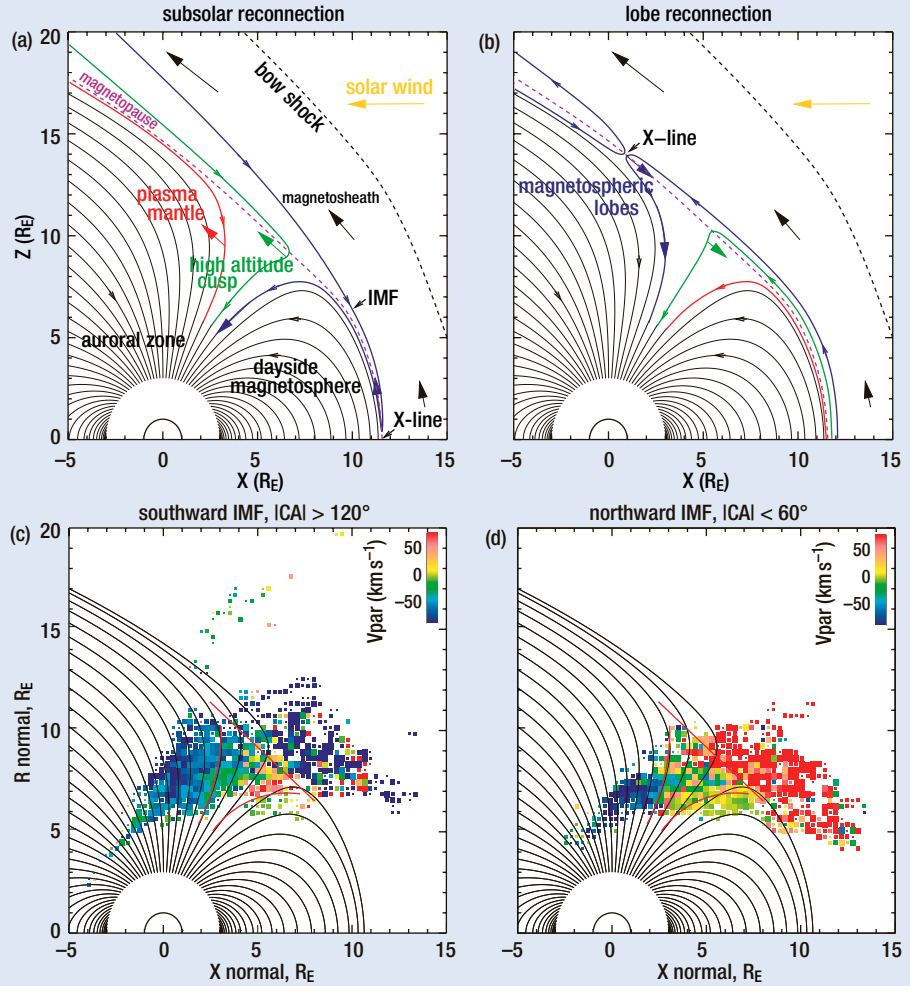

3: Panels (a) and (b) show schematically the large-scale structure of the magnetic field topology and of the plasma flows in the high-altitude cusp and surrounding regions for (a) southward and (b) northward IMF directions. The location of the X-line is indicative of an approximate location of the reconnection process for both IMF geometries. The dashed purple (black) line is the approximate location of the magnetopause (bow shock) and the coloured arrows are indicative of the plasma flow directions expected for each case (yellow: solar wind; black: magnetosheath; blue: reconnection-associated; green and red: large-scale convection). The lower panels show spatial distributions of the field-aligned plasma flows in the high-altitude cusp region when IMF conditions are restricted to predominately (c) southward and (d) northward IMF orientations. The flow magnitude (in km s^{-1}) is shown by the colour palettes. The plasma data are averaged over bins of 0.3 R_E and the sizes of the squares are proportional to the number of samples but are saturated at the maximum (0.3 R_E) for more than 20 samples. The background field lines are calculated from the T96 magnetic field model; note that in the northern hemisphere magnetosphere, a parallel flow is directed earthward.

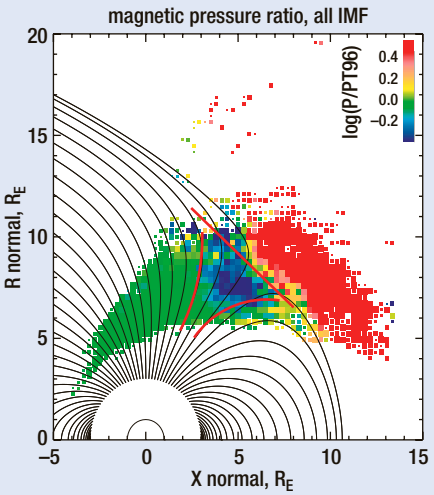

4: The spatial distribution of the ratio of the measured magnetic pressure ($B^2/2\mu_0$) to that calculated from the T96 model. The colour palette illustrates the amplitude of the magnetic pressure ratio with blue indicating a small measured magnetic pressure. In this figure all IMF conditions are taken into account. The three red lines surrounding the magnetic field cavity correspond to approximate boundaries of the exterior cusp. Other details are given in the caption for figure 3.

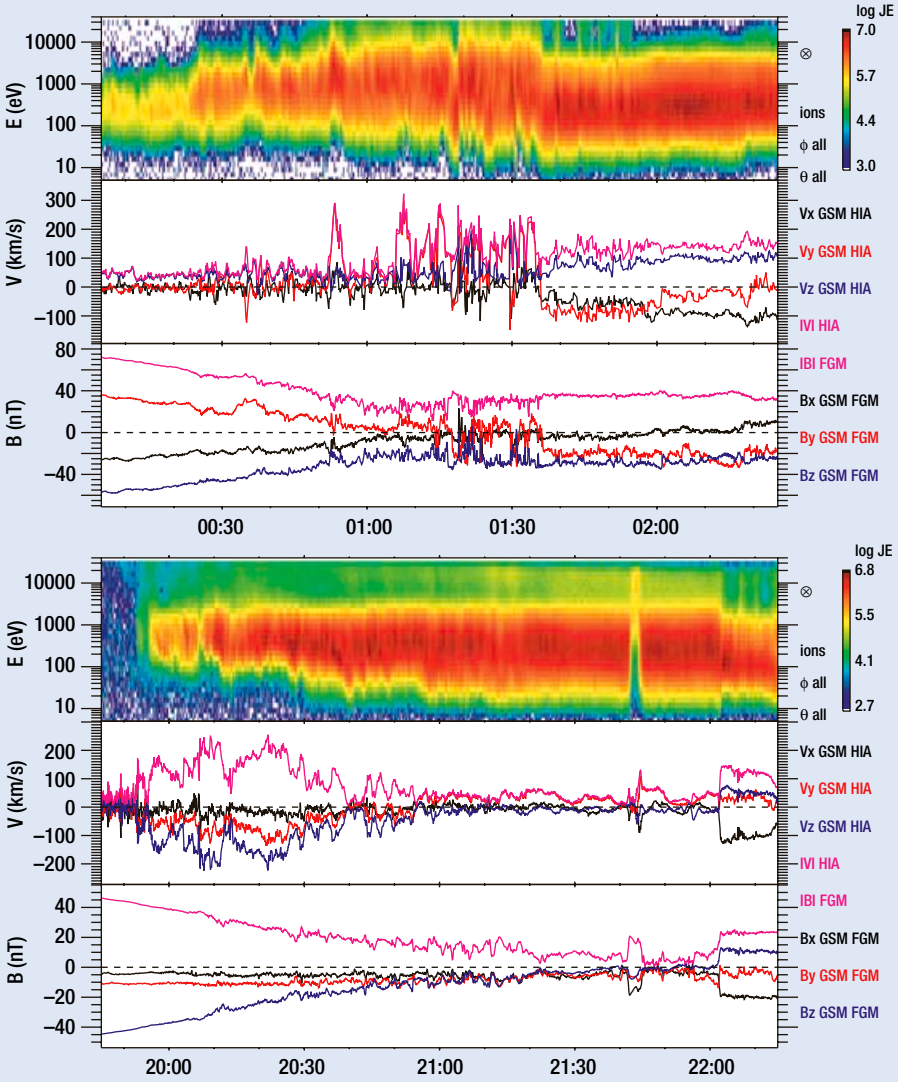

5: Cluster time-series of two selected outbound traversals of the high-altitude cusp region on 1 April 2003 for southward IMF (upper part) and on 4 February 2001 for northward IMF (lower part). The three panels show: the ion energy–time spectrogram, the ion velocity components, where all ions are assumed to be protons, and the magnetic field components. Magnetopause crossings are at 01:36 and 22:02 UT respectively for the two events.

plasma flow aligned with the magnetic field for southward and northward IMF orientations respectively (Lavraud *et al.* 2004b). For southward IMF, solar wind plasma penetrating the cusp flows earthward (parallel flows are red) and primarily at the equatorward side of the cusp (figure 3c). This is to be expected if there is magnetic reconnection at the low-latitude magnetopause (figure 3a). Although not shown here, the field-aligned flows are correlated with a large tailward convection (perpendicular flow), compatible with the scenario in figure 3a.

For northward IMF, no downward flows are observed at the equatorward edge of the cusp (figure 3d), but rather field-aligned downward flows are seen near the boundary with the lobes at higher latitudes. Although not shown, a slight sunward convection is also present near the poleward boundary of the cusp, correlated with the aforementioned flows. This time, the statistical properties of the region are compatible with magnetic reconnection at high latitudes, at the magnetopause in the lobes, as in figure 3b.

Structure of plasma flow: single event

To put these statistical results in context, we examine two individual Cluster encounters with the high-altitude cusp. Figure 5 displays Cluster data for two traverses of the northern cusp on 1 April 2003 and 4 February 2001, when the IMF was southward and northward respectively. At 00:05 UT on 1 April 2003, Cluster was in the plasma mantle characterized by predominantly up-flowing ions ($V_Z > 0$ in central panel). The mean energy of the ions (top panel) and their velocity gradually increased until 01:36 UT as the spacecraft moved towards higher altitudes and lower latitudes. This is consistent with the velocity filter effect (Lockwood and Smith 1992). The highest velocities were observed at the lowest latitudes and all the exterior cusp region had large ion speeds, mainly duskward and upward (V_Y and $V_Z > 0$). Cluster met the magnetopause at 01:36 UT. Such plasma properties suggest magnetic reconnection below the spacecraft, at the low-latitude magnetopause.

On 4 February 2001 Cluster first sampled a region basically void of plasma (top panel) until high-speed downward flows at 19:55 UT were detected ($V_Z < 0$ in middle panel). This is the northern magnetospheric lobe, so Cluster observed no plasma mantle. Large downward flows were detected at high magnetic latitudes, which, together with the absence of a plasma mantle, is consistent with magnetic reconnection at the lobes. Reversed velocity dispersion was then observed, with velocities gradually decreasing until about 21:30 UT, then staying low in the exterior cusp until 22:02 UT. This is consistent with the reversed plasma flow pattern in figure 3b for northward IMF and lobe reconnection. The spacecraft met the magnetopause at 22:02 UT and crossed the equatorward boundary of the exterior cusp at ~21:43 UT.

Boundary analysis

One of the major benefits of Cluster is the ability to combine data from the four spacecraft to determine the absolute motion of boundaries, as well as the sense and magnitude of flow. We focus on the magnetopause boundary at 22:02 UT on 4 February 2001, when the spacecraft separation was 600 km. Figure 6 shows the ion and magnetic field behaviour for a 5-minute interval around this boundary. The data are in a boundary-normal coordinate system determined using minimum variance analysis (MVA: Sonnerup and Cahill 1967) on magnetic field data from the four spacecraft. The top panel shows the ion velocity along the normal for spacecraft

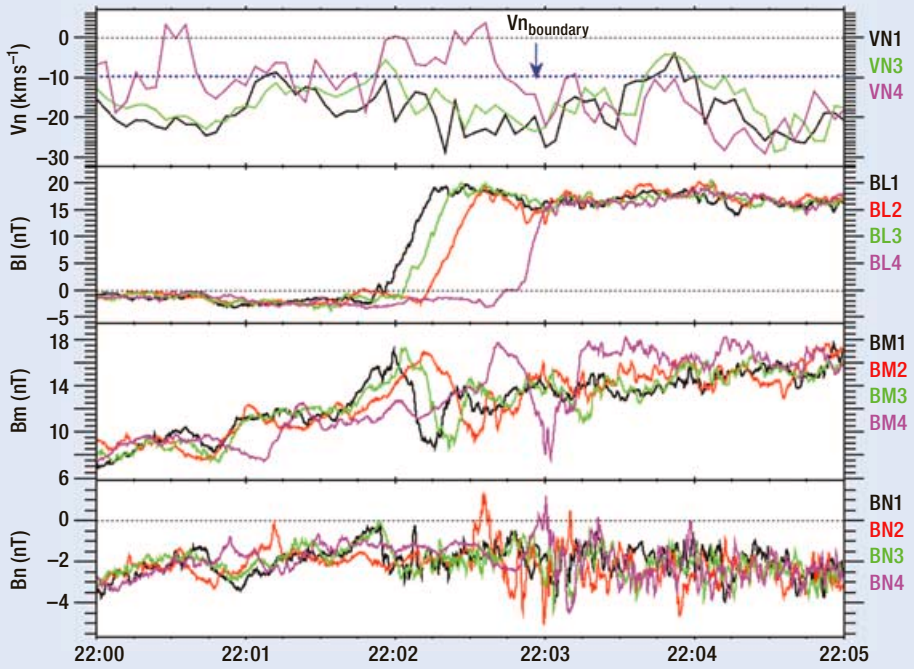

6: Cluster ion and magnetic field data from a short interval around the exterior cusp–magnetosheath (the magnetopause) boundary on 4 February 2001. The top panel shows the ion velocity component normal to the boundary for spacecraft 1, 3 and 4, with the actual normal speed of the boundary superimposed. The next three panels respectively show the maximum, intermediate and minimum variance components of the magnetic field estimated from the MVA analysis. A colour-coding is used for each of the four Cluster spacecraft: black (1), red (2), green (3) and magenta (4).

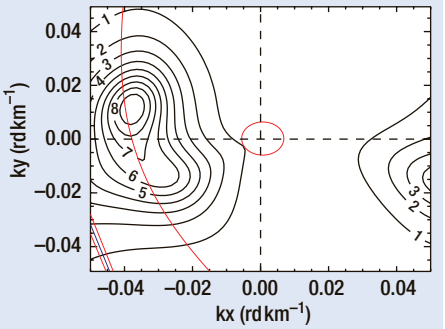

7: A superposition of the experimental magnetic energy density spectrum (black lines) and the theoretical dispersion relations of low-frequency modes (red lines) in the spacecraft frame for a frequency of 0.46 Hz. The blue line represents the Doppler shift w = k.v (or mirror mode). The main peak is consistent with an Alfvèn wave of frequency 0.21 Hz in the plasma frame.

1, 3 and 4. The panels below show the magnetic field in the maximum, intermediate and minimum (normal) directions for each Cluster craft.

Assuming a planar boundary, one can estimate its normal speed (Dunlop *et al.* 2003): ~−8.8 km s^{-1} inward in this case. Here the plasma flow across the boundary is slower than the boundary normal speed so that there is an actual plasma flow through the boundary. The boundary appears to be open, consistent with the entry of solar wind plasma into the exterior cusp – in turn, consistent with the boundary being the result of reconnection (Russell *et al.* 2000, Onsager *et al.* 2001, Lavraud *et al.* 2002).

Wave analysis

Cluster has made major advances in another field: wave propagation in collisionless plasmas, for which the cusp is a rewarding location. In many cases with northward IMF, downward-flowing plasma jets just inside the lobe boundary (presumably from lobe reconnection) are the site of bursts of low-frequency turbulence, often with peaks near the ion cyclotron frequency (Nykyri *et al.* 2003, Grison *et al.* 2004).

An interesting data set was obtained on 23 March 2002 when the spacecraft were 100 km apart (Grison *et al.* 2004). The k-filtering technique developed by Pinçon and Lefeuvre (1991), which requires an optimal tetrahedron geometry, can be applied here. This generalized minimum variance technique works like a telescope that can sense waves of any frequency and propagation direction. Magnetic field wave observations from the Cluster STAFF instrument (Cornilleau-Wehrlin *et al.* 2001) are used.

Figure 7 shows the resulting energy density spectrum for an interval of strong flows on 23 March 2002. A cut of the spectrum for $f_{S/C} = 0.46$ Hz (~f_{CI}) is shown using an isocontour representation ($f_{S/C}$ is the frequency in the spacecraft frame while f_{CI} is the ion cyclotron frequency). The most intense peak, in the top left quadrant of the distribution, corresponds to a wave vector at 88° to the ambient magnetic field. The corresponding frequency in the plasma frame ($f_{PLASMA} = f_{S/C} - \mathbf{k}.\mathbf{v}$) is about 0.21 Hz. The WHAMP program (Ronmark 1982) can then provide theoretical wave dispersion relations. The form of the energy density spectrum of the peak is consistent with the dispersion curve of the Alfvèn mode (red in figure 7).

Conclusions

The meeting showed the major advances obtained from Cluster on the structure of the high-altitude magnetospheric cusps. For the first time, the dominant role of magnetic reconnection in determining the large-scale cusp structure as a function of IMF orientation was made clear. Measured plasma and magnetic field properties are consistent with this interpretation, indicating that the cusps cannot be considered in isolation from the rest of the high-altitude magnetosphere. The overall topology of the cusp boundaries are now clear, as is their absolute motion, scale and whether plasma can penetrate them. Nonetheless, the Cluster data archive has only begun to be explored. In particular, very few cusp encounters have undergone a full study. While it is a reasonable expectation that the overall picture presented here will be sustained on further analysis, we should also expect surprises. ●

Benoit Lavraud, Los Alamos National Laboratory, USA. Peter J Cargill, Imperial College, London, UK.
Acknowledgments. The authors are grateful to Benjamin Grison and Nicole Cornilleau-Wehrlin for providing the k-filtering results presented here and also thank all Cluster teams for the hard work that made this science possible. PC acknowledges a PPARC senior research fellowship. Work at Los Alamos was conducted under the auspices of the US Department of Energy, with support from the NASA Cluster programme.

References

Balogh A *et al.* 2001 *Ann Geophys* **19** 1207.
Cargill P J 1999 *JGR* **104** 14 647.
Cornilleau-Wehrlin N *et al.* 2003 *Ann. Geophys* **21** 437.
Dunlop M W *et al.* 2003 *JGR* **107** doi:10.1029/2001JA005089.
Frank L A 1971 *JGR* **76** 5202.
Grison B *et al.* 2004 submitted to *Ann. Geophys*.
Haerendel G *et al.* 1978 *JGR* **83** 3195.
Heikkila W J and Winningham J D 1971 *JGR* **76** 883.
Lavraud B *et al.* 2002 *Geophys Res Lett* **29** doi:10.1029/2002GL015464.
Lavraud B *et al.* 2004a *Ann. Geophys* **22** 3009.
Lavraud B *et al.* 2004b *JGR* in press.
Lockwood M and Smith M F 1992 *JGR* **97** 14 841.
Newell P T and Meng C I 1988 *JGR* **93** 14 549.
Nykyri K *et al.* 2003 *Geophys Res Lett* **24** doi:10.1029/2003GL018594.
Onsager T G *et al.* 2001 *JGR* **106** 25 467.
Paschmann G *et al.* 1976 *JGR* **81** 2883.
Pinçon J-L and Lefeuvre F 1991 *JGR* **96** 1789.
Rème H *et al.* 2001 *Ann Geophys* **19** 1303.
Rönnmark K 1982 Kiruna Geophysical Institute Report 179.
Russell C T *et al.* 2000 *JGR* **105** 5489.
Sahraoui F *et al.* 2003 *JGR* **108** doi:10.1029/2002JA009587.
Sonnerup B U O and Cahill L J 1967 *JGR* **72** 171.
Tsyganenko N A 1996 **ESA SP-389** 181.